

Alma Mater Studiorum Università di Bologna  
Archivio istituzionale della ricerca

Quercetin loaded gelatin films with modulated release and tailored anti-oxidant, mechanical and swelling properties

This is the final peer-reviewed author's accepted manuscript (postprint) of the following publication:

*Published Version:*

Rubini K., Boanini E., Menichetti A., Bonvicini F., Gentilomi G.A., Montalti M., et al. (2020). Quercetin loaded gelatin films with modulated release and tailored anti-oxidant, mechanical and swelling properties. FOOD HYDROCOLLOIDS, 109, 1-9 [10.1016/j.foodhyd.2020.106089].

*Availability:*

This version is available at: <https://hdl.handle.net/11585/772373> since: 2020-09-21

*Published:*

DOI: <http://doi.org/10.1016/j.foodhyd.2020.106089>

*Terms of use:*

Some rights reserved. The terms and conditions for the reuse of this version of the manuscript are specified in the publishing policy. For all terms of use and more information see the publisher's website.

This item was downloaded from IRIS Università di Bologna (<https://cris.unibo.it/>).  
When citing, please refer to the published version.

(Article begins on next page)

This is the final peer-reviewed accepted manuscript of:

Rubini, K.; Boanini, E.; Menichetti, A.; Bonvicini, F.; Gentilomi, G. A.; Montalti, M.; Bigi, A. Quercetin Loaded Gelatin Films with Modulated Release and Tailored Anti-Oxidant, Mechanical and Swelling Properties. *Food Hydrocolloids* **2020**, *109*, 106089.

The final published version is available online at:  
<https://doi.org/10.1016/j.foodhyd.2020.106089>

#### Rights / License:

The terms and conditions for the reuse of this version of the manuscript are specified in the publishing policy. For all terms of use and more information see the publisher's website.

This item was downloaded from IRIS Università di Bologna (<https://cris.unibo.it/>)

**When citing, please refer to the published version.**

1        **Quercetin loaded gelatin films with modulated release and tailored**  
2        **anti-oxidant, mechanical and swelling properties**

3  
4        Katia Rubini<sup>a</sup>, Elisa Boanini<sup>a,\*</sup>, Arianna Menichetti<sup>a</sup>, Francesca Bonvicini<sup>b</sup>,  
5        Giovanna Angela Gentilomi<sup>b</sup>, Marco Montalti<sup>a</sup>, Adriana Bigi<sup>a</sup>

6  
7  
8        *<sup>a</sup> Department of Chemistry “Giacomo Ciamician”, University of Bologna, Via Selmi 2,*  
9        *40126 Bologna, Italy*

10        *<sup>b</sup> Department of Pharmacy and Biotechnology, University of Bologna, Via Massarenti*  
11        *9, 40138 Bologna, Italy*

12  
13  
14  
15        **Corresponding Author:**

16        \*Prof. Elisa Boanini; e-mail address: elisa.boanini@unibo.it

## Abstract

Quercetin, a flavonoid widely diffused in fruits and vegetables, is known for its good pharmacological qualities, such as anti-oxidant and anti-inflammatory properties. In this work, we loaded quercetin on gelatin films with the aim to develop materials with tailored anti-oxidant, mechanical and stability properties. To this purpose, gelatin films at increasing flavonoid content were prepared using two different solvents, namely H<sub>2</sub>O/EtOH (EtOH films) and DMSO (DMSO films). Quercetin content increased up to about 3.8 and 1.8 wt% in DMSO and EtOH films, respectively. The use of DMSO as solvent prevents the partial regain of collagen triple helix structure during gelling of gelatin sols and results in remarkable extensibility of the films. At variance, EtOH films display X-ray diffraction patterns and DSC plots in agreement with the presence of triple helix structure, and exhibit reduced swelling and increasing mechanical properties on increasing quercetin content. Moreover, their values of denaturation enthalpy indicate the presence of chemical interaction between the flavonoid and gelatin, which can be responsible of their lower quercetin release in PBS in comparison to DMSO films. The flavonoid release is sustained for both series of films and occurs through anchorage to gelatin nanoparticles. Moreover, both DMSO and EtOH functionalized films exhibit relevant anti-oxidant properties, in agreement with their RSA levels, which are comparable to that of pure quercetin.

**Keywords:** gelatin; quercetin; anti-oxidant properties; mechanical properties; fluorescence; swelling

## 1. Introduction

Gelatin is a renewable and biodegradable material (Chiellini, Cinelli, Corti, & Kenawy, 2001) which is obtained by chemical or thermal degradation of collagen. Its characteristics, including abundance, biocompatibility, low cost and absence of antigenicity, make gelatin an ideal raw material for food processing, packaging, as well as for pharmaceutical and biomedical applications. On the other hand, this biopolymer exhibits poor mechanical and water vapor barrier properties. In fact, gelatin is highly soluble in aqueous solutions, which limits most of its potential applications. Improvement of gelatin films functionality is usually achieved through crosslinking with chemical agents or through physical treatments. Dehydrothermal treatment, U.V. and gamma irradiation are the most frequent utilized physical methods, whereas chemical agents include dialdehydes, diisocyanates, genipin, carbodiimides, acyl azide, polyepoxy compounds, oxidized alginate and transglutaminase (Amadori et al., 2015; Boanini, Rubini, Panzavolta, & Bigi, 2010; Kolodziejska, & Piotrowska, 2007; Kuijpers et al., 1999; Rault, Frei, Herbage, Abdul-Malak, & Huc, 1996; Sung, Huang, Chang, Huang, Hsu, 1999; van Wachem et al., 1999).

Generally speaking, protein crosslinking can also be achieved through reaction of their side chain amino groups with polyphenols (Hosseini, & Gómez-Guillén, 2018; Strauss, & Gibson, 2004). These compounds, widespread in fruits, vegetable and seeds, are potent anti-oxidants and are receiving increasing interest thanks to their health beneficial properties, including anti-carcinogenic, anti-thrombotic, anti-inflammatory, anti-microbial, vasodilatory effects (Ozdal, Capanoglu, & Altay, 2013). Furthermore, polyphenols can stimulate osteoblast proliferation and activity and, as a consequence, promote bone formation and mineralization (Shavandi et al., 2018). Their interactions with proteins have been suggested to involve hydrogen bonding, ionic and hydrophobic interactions and covalent bonding (Hosseini et al., 2018; Zhang et al., 2010). Several

72 studies indicate that crosslinking gelatin films with polyphenolic compounds, including  
73 green tea polyphenols, rosemary and oregano extracts, caffeic, ferulic and gallic acids,  
74 provide materials with improved mechanical parameters and anti-oxidant properties  
75 (Chen et al., 2017; Gómez-Estaca, Bravo, Gómez-Guillén, Alemán, & Montero, 2009;  
76 Zhang et al., 2010). Herein, we studied the modifications of the properties of gelatin  
77 films induced by one of the most abundant flavonoids, namely quercetin (3,3',4',5,7-  
78 pentahydroxy-flavone). Quercetin has remarkable anti-oxidant, anti-inflammatory, anti-  
79 bacterial and anti-cancer effects. In particular, it has been shown to inhibit the  
80 proliferation of different types of cancer cells (Wang et al., 2016). On the other hand, its  
81 low water solubility and poor oral bioavailability limits its efficacy in dietary and  
82 pharmaceutical applications. These drawbacks have stimulated the research of possible  
83 systems for local delivery of the flavonoid (Forte et al., 2016; Forte et al., 2017; Patel,  
84 Heussen, Hazekamp, Drost, & Velikov, 2012; Zhang, Yang, Tang, Hu, & Zou, 2008).  
85 In this study, we developed gelatin films added with increasing amounts of quercetin,  
86 with the purpose to enrich the films with the peculiar functionalities of quercetin and, at  
87 the same time to modulate the mechanical and swelling properties of the films. Since  
88 quercetin is moderately soluble in ethanol and highly soluble in dimethyl sulfoxide  
89 (DMSO), the films were prepared following different routes, which imply the use of  
90 water/ethanol or DMSO, as solvents.

## 2. Materials and Methods

### 2.1 Preparation of the films

#### 2.1.1 Direct syntheses

Gelatin from pig skin (280 Bloom, Italgelatine S.p.A.) was used: 5 g of gelatin were dissolved in 100 ml of a mixture of water/ethanol (50/50) or in 100 ml of pure dimethyl sulfoxide (DMSO) at 40°C for about 30 min. Films were obtained on the bottom of Petri dishes (diameter = 6 cm) from 7.4 ml of gelatin solution after solvent evaporation: water/ethanol at room temperature, DMSO at 45 °C. Complete drying was attained under laminar flow hood.

Gelatin-quercetin films were obtained following the above procedure, and adding quercetin powder to gelatin before solvent addition. Different amounts of quercetin were used: 0.5, 1, 1.5 and 2 g/l.

Therefore samples prepared in water/ethanol and in DMSO were respectively labeled as W 05, W 1, W 15, W 2 and DMSO 05, DMSO 1, DMSO 15, DMSO 2.

Similarly, reference samples with no quercetin were labeled W 0 and DMSO 0.

#### 2.1.2 Preparation by adsorption

Since direct synthesis in water/ethanol (50/50) provoked precipitation of quercetin in solution, water/ethanol was used as a solvent following an adsorption procedure. In this case, 5 g of gelatin were dissolved in 100 ml of water at 40°C for about 30 min. Films were obtained on the bottom of Petri dishes (diameter = 6 cm) from 7.4 ml of gelatin solution after solvent evaporation at room temperature. Before complete drying, 7.4 ml of a solution of quercetin in water/ethanol (50/50) was placed into each Petri dish for 24 hours. Afterwards films were washed with distilled water and completely dried under laminar flow hood.

Different amounts of quercetin were used: 0.5, 1, 1.5 and 2 g/l. Therefore samples prepared by adsorption of quercetin were respectively labelled as EtOH 05, EtOH 1, EtOH 15, EtOH 2, whereas reference sample with no quercetin was labeled EtOH 0.

## **2.2 Characterization of the films**

### **2.2.1 Quercetin content and quercetin release**

Quercetin content was determined on samples dissolved in H<sub>2</sub>O/EtOH 1:1 solution at a concentration of 20 mg/mL and maintained at 40°C for one day. Absorption spectra of each series of films were collected on 1:50 diluted film solutions (0.4 mg/mL) .

Quercetin release was determined on samples (1cmx1cm) placed at the bottom of a vial and added with 5 mL of PBS 0.1M (pH 7.4). The release was monitored for 10 hours at room temperature, collecting absorption spectra on supernatant diluted 1:1 with Ethanol. The spectra were recorded at selected times and the PBS solution was refreshed after each absorbance measurement.

Absorption spectra were collected with a Perkin Elmer UV/Vis spectrometer Lambda 45. Quercetin content of the films, as well as quercetin release, was obtained by means of Lambert-Beer law:

$$Abs = \varepsilon \cdot b \cdot c$$

where *Abs* is the Absorbance,  $\varepsilon$  [M<sup>-1</sup>cm<sup>-1</sup>] is the extinction molar coefficient, *b* [cm] is the optical path (1cm) and *c* [M] is the concentration of quercetin.

For the evaluation of quercetin content, the molar extinction coefficient (15360 M<sup>-1</sup> cm<sup>-1</sup>) was calculated by collecting absorption spectra of known quantities of quercetin dissolved in a water/ethanol 1:1 mixture containing gelatin (0.4 mg/mL).

For the evaluation of quercetin release, the molar extinction coefficient (14234 M<sup>-1</sup> cm<sup>-1</sup>) was calculated by collecting absorption spectra of known quantities of quercetin dissolved in a PBS 0.1M/ethanol 1:1 mixture.



#### 2.2.2 *Dynamic light scattering analysis*

Dynamic light scattering DLS (Malvern Zetasizer Nano-ZS) was performed on DMSO 15 and EtOH 15 samples, compared to the reference samples (DMSO 0 and EtOH 0). Samples of about 1 cm<sup>2</sup> were placed on the bottom of a vial, added with 5 mL of PBS and kept at 25°C for 1 hour. After 1 hour the supernatant solution was collected for DLS characterization. When possible, the solutions were filtered by means of an RC 0.45µm filter.

#### 2.2.3 *Steady state fluorescence anisotropy measurements*

Steady state fluorescence anisotropy analysis was performed (Edinburgh Instrument) using a 380 nm LED light to excite quercetin. Emission spectra were recorded from 400 nm to 700 nm.

#### 2.2.4 *Fluorescence microscopy*

Transmission and fluorescence images were obtained by a fluorescence microscope (Olympus IX71) with a 10x objective. In order to collect the fluorescence images, excitation was performed at 378-400 nm and the fluorescence was observed at 510-542 nm.

#### 2.2.5 *Thermal analyses*

Calorimetric measurements were performed using a Perkin Elmer Pyris Diamond differential scanning calorimeter equipped with a model ULSP 90 intra-cooler. Temperature and enthalpy calibration was performed by using high-purity standards (n-decane and indium). The measurements were carried out on dried samples, hermetically sealed in aluminium pans. Heating was carried out at 5 °C min<sup>-1</sup> in the temperature range from 40 °C to 120 °C. Denaturation temperature was determined as the peak value of the corresponding endothermic phenomena. The value of denaturation enthalpy was calculated with respect to the sample weight.

Thermogravimetric analysis was performed using a Perkin–Elmer TGA-7, heating samples (5–10 mg) in a platinum crucible in air flow (20 cm<sup>3</sup>/min) at a rate of 10 °C/min up to 800 °C.

#### 2.2.6 X-ray diffraction

X-ray diffraction analysis was carried out by means of a Panalytical XCellerator powder diffractometer. Cu K $\alpha$  radiation was used (40 mA, 40 kV). The 2 $\theta$  range was from 5° to 40° with a step size of 0.1° and time per step of 200 s.

#### 2.2.7 Swelling, water solubility and contact angle

For swelling experiments films were cut into portion 1 cm x 1cm and were weighted in air-dried conditions. Then they were immersed in phosphate-buffered saline (PBS, 0.1 M) solution for different periods of time. Wet samples were wiped with filter paper to remove excess liquid and weighed. The amount of absorbed water was calculated as

$$W(\%) = [(W_w - W_d)/W_d] \cdot 100$$

where  $W_w$  and  $W_d$  are the weights of the wet and the air-dried samples.

Water solubility was determined in triplicate (Giménez, Gómez-Estaca, Alemán, Gómez-Guillén, & Montero, 2009). Portions of the films (2x2 cm) were placed into glass containers with 15 ml of distilled water and subjected to gentle shaking at 65 rpm for 15 h at 22°C. Filtration on filter paper was used to recover the remainder of the undissolved film, which was desiccated at 105°C for 24 h. The film solubility was calculated as

$$FS(\%) = [(W_0 - W_f)/W_0] \cdot 100$$

where  $W_0$  is the initial weight of the film expressed as dry matter and  $W_f$  is the weight of the desiccated undissolved rest of the film.

Static contact angle measurements were performed on films using a KSV CAM-101 instrument under ambient conditions. The side profiles of deionized water drops were

recorded for image analysis in a time range of 0–10 s, by collecting an image every 0.5 s. At least three drops were observed for each sample.

#### 2.2.8 Mechanical tests

For mechanical tests, films prepared by direct synthesis in DMSO or by adsorption from water/ethanol were immersed into a mixture of water/ethanol (in the ratio 2:3) for 1 min or 72 h respectively.

Stress–strain curves of strip-shaped (3 mm x 30 mm, thickness around 0.12 mm) films were recorded using an INSTRON Testing Machine 4465, with a crosshead speed of 5 mm min<sup>-1</sup>, and the Series IX software package. The thickness of the samples was determined using a Leitz SMLUX- POL microscope. The Young's modulus  $E$ , the stress at break  $\sigma_b$  and the strain at break  $\varepsilon_b$  of the strips were measured.

Statistical analysis was performed with the Student  $t$ -test considering a  $p$  value of less than 0.05 to be significantly different.

#### 2.2.9 Radical Scavenging Assay

Antioxidant activity was determined on the basis of quercetin ability to act as radical scavengers toward the stable 2,2-diphenyl-1-picrylhydrazyl free radical, (DPPH•) (Sigma). Solutions of EtOH 1, EtOH 2, DMSO 1 and DMSO 2 were prepared by dissolving the solid samples in MilliQ water/EtOH at 40 °C, thereafter they were diluted, basing on their known quercetin contents, in order to get 10, 30 and 50  $\mu$ M of quercetin concentrations. Dilutions of pure quercetin (Sigma), 10, 30 and 50  $\mu$ M, were prepared and used as reference samples. For the assay, 50  $\mu$ L of each solution (samples and references) were added to 3 mL of DPPH• saturated ethanol/water (20/80 V/V) solution, previously clarified by centrifugation (10000 rpm for 10 minutes). After an incubation of 10 minutes at room temperature in darkness, absorbance values ( $A$ ) were spectrophotometrically measured at 517 nm. The radical scavenging activity (RSA) was determined through the following equation:

224        $\% \text{ RSA} = (A_0 - A_x)/A_0 \times 100$

225       where  $A_0$  is the absorbance of the control (containing DPPH• solution without  
226       quercetin), and  $A_x$  is the absorbance in the presence of quercetin (as reference) or of  
227       quercetin-containing samples.

228       Statistical evaluation of data was performed using GraphPad Prism version 5.00 for  
229       Windows (GraphPad Software). One-way analysis of variance (ANOVA) followed by  
230       Dunnett's Multiple comparison test was used to determine significance of differences  
231       ( $p < 0.05$ ) among experimental groups and reference samples.

#### 232       2.2.10 Antibacterial properties of films

233       The *in vitro* antibacterial activity of the films was evaluated against *Staphylococcus*  
234       *aureus* (ATCC 25923) and *Escherichia coli* (ATCC25922) selected as controls and  
235       representative strains for Gram positive and Gram negative bacteria. The effectiveness  
236       of samples to inhibits bacterial growth was assessed by a standardized Kirby-Bauer  
237       (KB) diffusion test on Mueller-Hinton agar plate and by measuring the bacterial-free  
238       zone around the disk-shaped samples ( $\varnothing = 6 \text{ mm}$ ) after 24h of incubation at 37°C.

239       In addition, the films were assayed for their antibacterial activity following incubation  
240       in PBS, at pH 7.4 and at 37°C to mimic physiological environment. For this purpose,  
241       each film was prepared in a vial and incubated with 200  $\mu\text{L}$  of PBS. Then, the liquid  
242       samples, containing released quercetin from the different films, were evaluated against  
243       *S. aureus* and *E. coli* by means of a broth microdilution method using a 96-well plate  
244       (Boanini, et al. 2018). In parallel, pure quercetin dissolved in DMSO at 30 mg/mL was  
245       assayed against *S. aureus* and *E. coli* in the range 500 – 15.625  $\mu\text{g/mL}$ . Bacterial growth  
246       was determined by measuring the absorbance value ( $A$ ) at 630 nm (OD) and the  
247       effectiveness of the quercetin, as pure compound and released from the film samples,  
248       was expressed as percentage value relative to the positive growth control (bacterial  
249       suspension in regular medium).

All experiments were performed on duplicate in different days, using gentamicin disk (10  $\mu\text{g}$ ) or gentamicin solution (in the range 5  $\mu\text{g/mL}$  to 0.005  $\mu\text{g/mL}$ ,) as reference drug.

### **3. Results and discussion**

Quercetin functionalized gelatin films display different properties depending on the preparation process. The use of DMSO as solvent allowed to dissolve gelatin and quercetin in the same solution and to obtain films at different content of the flavonoid (DMSO films). At variance, the films prepared in water/ethanol (W films) were opaque and not homogeneous due to the precipitation of quercetin (Figure S1).

Therefore, we followed an alternative route where air-dried films prepared from gelatin aqueous solution were maintained in contact with quercetin dissolved in water/ethanol for 24 hours (EtOH films).

#### ***3.1 Quercetin content***

The amount of quercetin incorporated in the functionalized films was determined through evaluation of absorption spectra of films dissolved in a water/ethanol mixture (Figure 1).

The data of quercetin concentration in the solutions of the different samples were utilized to calculate quercetin content of the films (Table 1).

The results reported in Table 1 show that the two film preparation methods lead to different amounts of quercetin loading. Quercetin content of DMSO films corresponds to that present in the preparation solution, as expected. On the contrary, the preparation procedure of EtOH samples implies quercetin adsorption from solution after preparation of the gelatin films, which yields a lower flavonoid content in the final films.

### 3.2 Fluorescence microscopy

Quercetin distribution inside the films was evaluated through fluorescence of the films (Figure S2). The results show that quercetin is homogeneously distributed in DMSO film, whereas its distribution in ETOH films seems not completely uniform, as shown in Figure S2: although the comparison of the image of EtOH 1 with that of EtOH 0 shows that the flavonoid is distributed all through the film, there are regions where it is more densely packed. Fluorescence microscope images confirm the particular distribution of quercetin in the films, as shown in Figure S3 for EtOH 1, which involves the formation of quercetin fluorescent aggregated structures of various sizes (from 20-30  $\mu\text{m}$  to 80-90  $\mu\text{m}$ ).

### 3.3 Thermogravimetric analysis

The results of thermogravimetric analysis confirm the greater quercetin content of DMSO than EtOH films. The TG plots of all the samples are characterized by three weight losses: the first (between about 30 and 250°C) corresponds to water loss; the second (between about 250 and 500°C) is due to gelatin decomposition; the third one (centered around 600-700°C) is due to combustion of the residual components (Bigi, Panzavolta, & Rubini, 2004a). Quercetin decomposition occurs around 350°C (Borghetti et al., 2012), that is in the same region of gelatin decomposition. Figure 2 reports the TG plots of the EtOH 2 and DMSO 2 samples compared with those of the relative controls. The comparison of the different weight losses in the range of temperature 250-500°C indicate that quercetin content in EtOH 2 and DMSO 2 films is about  $1\pm 1$  and  $3\pm 1$  wt% respectively (Table S1), in good agreement with absorbance results. Moreover, the results of thermogravimetric analysis demonstrate that the films do not contain any residual solvent. In particular, the absence of DMSO is supported also by the results of FTIR analysis: the spectrum of DMSO is characterized by a strong band at 102  $\text{cm}^{-1}$ , which is not present in the spectra of DMSO films, as shown in Figure

S4. It is also worth noticing that the temperature corresponding to complete combustion is higher for the samples containing quercetin (745 and 726°C respectively for EtOH 2 and EtOH 0; 770 and 758°C for DMSO 2 and DMSO 0), suggesting a stabilizing effect of the flavonoid.

### ***3.4 Swelling, water solubility and contact angle***

The incorporation of quercetin in EtOH films resulted in reduced values of swelling in phosphate buffer (Figure 3): swelling of pure gelatin films is about 1700% after 48 h immersion in PBS and decreases as a function of quercetin content down to 1000% for EtOH films at the maximum quercetin content. The degree of swelling of gelatin films prepared in DMSO is significantly lower: the maximum values reached by DMSO 0 and DMSO 2 films are about 700% and 600% respectively. However, the stability of the DMSO films in PBS is significantly reduced in comparison to that of EtOH films, so that after 48 h they are completely dissolved. Although also this series of films display a clear contribution of quercetin, the noticeable reduction of swelling induced by DMSO does not allow to appreciate a clear trend as a function of the content of the flavonoid.

At variance with swelling results, the values of contact angle and of water solubility of the different samples do not exhibit significant differences. In particular, contact angle displays mean values in the range 72°-77°, showing that all prepared films have a hydrophilic behavior and a good wettability (Table S2). Although DMSO films are less stable than EtOH films in PBS, they show similar water solubility, indeed FS (%) values do not vary even as a function of quercetin content, as reported in Table S4.

### ***3.5 Differential scanning calorimetry***

DSC analysis provides information on the thermal stability of gelatin and on its content of triple helical structure. In fact, cooling of gelatin aqueous solutions results in a partial renaturation of collagen structure which implies a partial recovery of the triple helix structure (Gómez-Guillén, Giménez, López-Caballero, & Montero, 2011). The DSC

plot of gelatin exhibits an endothermic peak due to the transition of the recovered portions of triple helix to random coils (denaturation), with an associated denaturation enthalpy which depends on the extent of triple helix structure (Bigi, Panzavolta, & Rubini, 2004b).

The DSC plot of EtOH 0 shows indeed the presence of an endothermic peak centered at about 100°C (denaturation temperature,  $T_d$ ) with an associated denaturation enthalpy ( $\Delta H_d$ ) of about 28 J/g (Table 2). Loading of quercetin in the EtOH films does not significantly affect their thermal stability, in agreement with the values of the denaturation temperature which do not vary significantly with composition (Table 1). At variance, the values of denaturation enthalpy of EtOH films containing quercetin are drastically reduced when compared with that of the unloaded sample, although it is not possible to appreciate variations as a function of quercetin content due to the broadening of the peaks (Figure 4, Table 2). Reduction of the value of gelatin denaturation enthalpy is usually observed on samples treated with crosslinking chemical agents and can be ascribed to a reduction of hydrogen bonds (which break endothermically) and/or to an increase of covalent crosslinks (which break exothermically) (Bigi et al., 2004b, Finch, & Ledward, 1972). On this basis, the observed decrease of denaturation enthalpy suggests possible chemical interactions between gelatin and quercetin molecules which stabilize the films, in agreement with the observed reduction of the degree of swelling. The DSC plot of quercetin films prepared from DMSO solution did not show any endothermic peak indicating absence of triple helix structure and suggesting that gelatin does not gelify in DMSO (Kozlov, & Burdigina, 1983).

### ***3.6 X-ray diffraction analysis***

In agreement with DSC results, the X-ray diffraction patterns of DMSO films show only a broad peak centered at about 20° of  $2\theta$ , corresponding to a periodicity of about 0.45 nm, which has been ascribed to the distance between adjacent polypeptide strands



of gelatin (Okuyama, 2008), confirming that DMSO prevents the partial renaturation of the protein. At variance, the XRD patterns of EtOH films exhibit also a sharp peak at about  $7^\circ$  of  $2\theta$  corresponding to a periodicity of about 1.1 nm and related to the diameter of the triple helix (Okuyama, 2008), as shown in Figure 5.

### ***3.7 Mechanical properties***

The absence of triple helix structure in the DMSO films can be considered responsible of their mechanical behavior, which is quite different from that of EtOH films. At variance with EtOH films, DMSO films cannot be maintained in the mixture water/ethanol for the period of time (72 h) usually utilized to reach a constant relative humidity of 75% (Boanini et al., 2010), and must be removed from the mixture just after 1 min because they become sticky. Moreover, under tensile stress, they undergo a remarkable elongation and exhibit jagged stress-strain curves (Figure S5), which prevent a proper evaluation of their mechanical parameters.

On the contrary, the stress strain curves of the samples of the EtOH series are similar to those characteristic of gelatin films (Amadori, et al. 2015), as shown from the comparison of a few typical curves of films at different quercetin content reported in Figure 6. The values of the Young's modulus,  $E$ , the stress at break,  $\sigma_b$ , and the deformation at break,  $\epsilon_b$ , for the different samples are reported in Table 3. Both the values of stress at break and deformation increase significantly on increasing quercetin concentration up to 1.5 g/L, whereas the value of Young's modulus does not show any significant variation. On the other hand, quercetin concentration of 2 g/L, which means a flavonoid content of 1.8 wt% (Table 1), provokes a significant worsening of the mechanical parameters of the films, as shown in Table 3, most likely also due to the non homogeneous distribution of the flavonoid inside the films.

### 3.8 Quercetin release

Quercetin release in PBS from some selected functionalized films was determined from absorbance values at the quercetin maximum (375 nm) as a function of time.

The results reported in Figure 7 show that the release initially increases with time, but reaches a steady state in a few hours. The amount of quercetin released by EtOH films is significantly lower than that liberated by DMSO films (maximum value of release : about 45 and 70 % of the initial content from EtOH and DMSO samples, respectively). Moreover, the percentage of quercetin release from DMSO films generally increases with quercetin content (with the exception of DMSO 1 sample), whereas EtOH samples display an opposite trend. The decrease of quercetin release from EtOH films on increasing their pristine content is in agreement with their swelling behavior and confirms the stabilizing role of the flavonoid, as suggested by the results of denaturation enthalpy.

Quercetin is not soluble in aqueous solutions (Zhang et al., 2008); however, quercetin release in PBS aqueous solution yields very clear and transparent solutions, suggesting that the flavonoid is actually released anchored to gelatin nanoparticles, which enhances its solubility. This process was studied in DMSO 15 and EtOH 15 samples through DLS analysis and fluorescence anisotropy measurements on the supernatant solution after quercetin release for 1 hour.

DLS measurements allow to detect the presence of nanoparticles in solution during the release (Montalti, Battistelli, Cantelli, & Genovese, 2014). The results of DLS analysis (Table S4) indicate that functionalized films, as well as EtOH 0 film, release nanoparticles with a diameter of about 30 nm. The release solution of DMSO 0 sample cannot be filtered, most likely because of a significant presence of gelatin in solution, and gave a result in agreement with a polydisperse solution with average size of almost 160 nm.

Fluorescence anisotropy measurements give information about the rotational freedom of the emitting molecules (Rampazzo et al., 2018). The supernatant solutions of the films (Figure S6) gave high values of mean anisotropy (0.21 and 0.15 for DMSO 15 and EtOH 15 respectively) indicating the presence of anisotropy in both DMSO 15 and EtOH 15 samples. This means that quercetin molecules in the solution experience limited rotational mobility and their fluorescence is thus partially polarized, which would confirm that quercetin is released through anchorage to gelatin nanoparticles

### ***3.9 Radical scavenging activity***

Quercetin can quench reactive oxygen species (ROS) displaying antioxidant activity (Enoki et al., 2014). ROS are involved in a number of pathologies, including not just inflammation but also cardiovascular diseases and cancer (Enoki et al., 2014; Obrenovich et al., 2011). Therefore, it is important to verify if quercetin functionalized gelatin films display the antioxidant properties of the flavonoid. To this aim, we tested the radical scavenging activity (RSA) of the different samples by means of the 1,1-diphenyl-2-picryl-hydrazyl (DPPH•) assay (Berlier et al., 2013; Mohan, Birari, Karmase, Jagtap, & Kumar Bhutani, 2012). DPPH• exhibits a characteristic absorption band at 515 nm. The intensity of this band can be reduced by the scavenging action of the antioxidant material, which donates hydrogen to DPPH• to form the corresponding hydrazine. The test was carried out on different amounts of samples in order to get different concentration of quercetin. The results show that RSA increases as a function of quercetin concentration. In particular, pure quercetin exhibits RSA values up to about 35% as its concentration increases up to 50  $\mu$ M. The data reported in Figure 8 show that all the examined samples display RSA values similar to those recorded for pure quercetin, indicating that the antioxidant properties is maintained in both series of functionalized films. No statistically significant differences were measured in RSA

values comparing the pure quercetin, set as reference control, and the tested samples at the same quercetin content, irrespective of the solvent used for preparation.

### **3.10 Antibacterial activity**

The antibacterial properties of the gelatin-quercetin-films, and of the quercetin released from the films following incubation in PBS, were evaluated by means of a standardized Kirby-Bauer disk diffusion test and a broth microdilution methodology, respectively. Despite the antimicrobial activity of quercetin against different bacterial strains has been previously demonstrated (Bonvicini et al., 2017), the gelatin-quercetin films obtained in the present study show no activity towards *S. aureus* and *E. coli*, irrespective of the assay used. The result could be ascribed to the low quercetin content of the films. Considering the highest quercetin amount loaded on the film samples (3.8%, see Table 1), and the weight of gelatin-quercetin films ( $5.39 \pm 1.80$  mg), none of the samples contained the Minimum Inhibitory Concentration (MIC) of quercetin enabling bacterial growth arrest. Indeed, the maximum amount of quercetin in the PBS solution tested in the broth microdilution assay was 20  $\mu\text{g/mL}$  while the MIC values for pure quercetin measured 125  $\mu\text{g/mL}$  and 500  $\mu\text{g/mL}$  for *S. aureus* and *E. coli*, respectively.

## **4. Conclusions**

The two different methods of preparation developed in this work provide functionalized films characterized by different properties. In particular, DMSO films are less stable in aqueous solution and display a very high extensibility, which hinders the measurement of their mechanical properties, most likely because they lack triple helix structure. The increase of quercetin content in EtOH films provokes a reduction of swelling degree, an increase of the mechanical parameters and a reduction of the denaturation

enthalpy, in agreement with the presence of chemical interaction between gelatin and the flavonoid. Most importantly, both quercetin containing DMSO and EtOH films show a sustained, gelatin nanoparticles mediated, flavonoid release in PBS, as well as RSA values indicative of remarkable anti-oxidant properties, suggesting possible applications as local delivery systems of the functionalizing agent.

## Acknowledgments

The authors are grateful to the support of the University of Bologna.

## Conflict of Interest

The authors have no competing interests to declare.

## References

- Amadori, S., Torricelli, P., Rubini, K., Fini, M., Panzavolta, S., & Bigi, A. (2015). Effect of sterilization and crosslinking on gelatin films. *Journal of Materials Science: Materials in Medicine*, 26, 69. (9 pp) <https://doi.org/10.1007/s10856-015-5396-4>
- Berlier, G., Gastaldi, L., Ugazio, E., Miletto, I., Iliade, P., & Sapino, S. (2013). Stabilization of quercetin flavonoid in MCM-41 mesoporous silica: positive effect of surface functionalization. *Journal of Colloid and Interface Science*, 393, 109–118. <https://doi.org/10.1016/j.jcis.2012.10.073>
- Bigi, A., Panzavolta, S., & Rubini, K. (2004)a. Relationship between triple helix content and mechanical properties of gelatin films. *Biomaterials*, 25, 5675–5680. <https://doi.org/10.1016/j.biomaterials.2004.01.033>
- Bigi, A., Panzavolta, S., & Rubini, K. (2004)b. Setting mechanism of a biomimetic bone cement. *Chemistry of Materials*, 16, 3740-3745. <https://doi.org/10.1021/cm049363e>

- Boanini, E., Rubini, K., Panzavolta, S., & Bigi, A. (2010). Chemico-physical characterization of gelatin films modified with oxidized alginate. *Acta Biomaterialia*, 6, 383–388. <https://doi.org/10.1016/j.actbio.2009.06.015>
- Boanini, E., Torricelli, P., Bonvicini, F., Cassani, M. C., Fini, M., Gentilomi, G. A., & Bigi, A. (2018). A new multifunctionalized material against multi-drug resistant bacteria and abnormal osteoclast activity. *European Journal of Pharmaceutics and Biopharmaceutics*, 127, 120–129. <https://doi.org/10.1016/j.ejpb.2018.02.018>
- Bonvicini, F., Antognoni, F., Mandrone, M., Protti, M., Mercolini, L., Lianza, M., Gentilomi, G. A., & Poli, F. (2017) Phytochemical analysis and antibacterial activity towards methicillin-resistant *Staphylococcus aureus* of leaf extracts from *Argania spinosa* (L.) Skeels. *Plant Biosystems*, 151, 649–656. <https://doi.org/10.1080/11263504.2016.1190418>
- Borghetti, G. S., Carini, J. P., Honorato, S. B., Ayala, A. P., Moreira, J. C. F., & Bassani, V. L. (2012). Physicochemical properties and thermal stability of quercetin hydrates in the solid state. *Thermochimica Acta*, 539, 109–114. <https://doi.org/10.1016/j.tca.2012.04.015>
- Chen, M., Liu, F., Chiou, B.-S., Sharif, H. R., Xu, J., & Zhong, F. (2017). Characterization of film-forming solutions and films incorporating free and nanoencapsulated tea polyphenol prepared by gelatins with different Bloom values. *Food Hydrocolloids*, 72, 381–388. <https://doi.org/10.1016/j.foodhyd.2017.05.001>
- Chiellini, E., Cinelli, P., Corti, A., & Kenawy, E. R. (2001). Composite films based on waste gelatin: thermal-mechanical properties and biodegradation testing. *Polymer Degradation and Stability*, 73, 549–555. [https://doi.org/10.1016/S0141-3910\(01\)00132-X](https://doi.org/10.1016/S0141-3910(01)00132-X)
- Enoki, Y., Sato, T., Tanaka, S., Iwata, T., Usui, M., Takeda, S., Kokabu, S., Matsumoto, M., Okubo, M., Nakashima, K., Yamato, M., Okano, T., Fukuda, T., Chida, D.,

- Imai, Y., Yasuda, H., Nishihara, T., Akita, M., Oda, H., Okazaki, Y., Suda, T., & Yoda, T. (2014). Netrin-4 derived from murine vascular endothelial cells inhibits osteoclast differentiation in vitro and prevents bone loss in vivo. *FEBS Letters*, 588, 2262–2269. <https://doi.org/10.1016/j.febslet.2014.05.009>
- Finch, A., & Ledward, D. A. (1972). Shrinkage of collagen fibers: a differential scanning calorimetric study. *Biochimica et Biophysica Acta*, 278, 433–439. [https://doi.org/10.1016/0005-2795\(72\)90003-7](https://doi.org/10.1016/0005-2795(72)90003-7)
- Forte, L., Torricelli, P., Boanini, E., Rubini, K., Fini, M., & Bigi, A. (2017). Quercetin and alendronate multi-functionalized materials as tools to hinder oxidative stress damage. *Journal of Biomedical Materials Research Part A*, 105A, 3293–3303. <https://doi.org/10.1002/jbm.a.36192>
- Forte, L., Torricelli, P., Boanini, E., Gazzano, M., Rubini, K., Fini, M., & Bigi, A. (2016). Antioxidant and bone repair properties of quercetin-functionalized hydroxyapatite: An *in vitro* osteoblast–osteoclast–endothelial cell co-culture study. *Acta Biomaterialia*, 32, 298–308. [doi:10.1016/j.actbio.2015.12.013](https://doi.org/10.1016/j.actbio.2015.12.013)
- Giménez, B., Gómez-Estaca, J., Alemán, A., Gómez-Guillén, M. C., & Montero, P. (2009). Physico-chemical and film forming properties of giant squid (*Dosidicus gigas*) gelatin. *Food Hydrocolloids*, 23, 585–592
- Gómez-Estaca, J., Bravo, L., Gómez-Guillén, M. C., Alemán, A., & Montero, P. (2009). Antioxidant properties of tuna-skin and bovine-hide gelatin films induced by the addition of oregano and rosemary extracts. *Food Chemistry*, 112, 18–25. <https://doi.org/10.1016/j.foodchem.2008.05.034>
- Gómez-Guillén, M. C., Giménez, B., López-Caballero, M. E., & Montero, M. P. (2011). Functional and bioactive properties of collagen and gelatin from alternative sources: a review. *Food Hydrocolloids*, 25, 1813–1827. <https://doi.org/10.1016/j.foodhyd.2011.02.007>

- Hosseini, S. F., & Gómez-Guillén, M. C. (2018). A state-of-the-art review on the elaboration of fish gelatin as bioactive packaging: Special emphasis on nanotechnology-based approaches. *Trends in Food Science & Technology*, 79, 125–135. <https://doi.org/10.1016/j.tifs.2018.07.022>
- Kolodziejska, I., & Piotrowska, B. (2007). The water vapour permeability, mechanical properties and solubility of fish gelatin-chitosan films modified with transglutaminase or 1-ethyl-3(3-dimethylaminopropyl) carbodiimide (EDC) and plasticized with glycerol. *Food Chemistry*, 103, 295–300. <https://doi.org/10.1016/j.foodchem.2006.07.049>
- Kozlov, P. V., & Burdigina, G. I. (1983). The structure and properties of solid gelatin and the principles of their modification. *Polymer*, 24, 651-666. [https://doi.org/10.1016/0032-3861\(83\)90001-0](https://doi.org/10.1016/0032-3861(83)90001-0)
- Kuijpers, A. J., Engbers, G. H. M., De Smedt, S. C., Meyvis, T. K. L., Demeester, J., Krijgsveld, J., Zaat, S. A. J., & Dankert, J. (1999). Characterization of the network structure of carbodiimide cross-linked gelatin gels. *Macromolecules*, 32, 3325–3333. <https://doi.org/10.1021/ma981929v>
- Mohan, R., Birari, R., Karmase, A., Jagtap, S., & Kumar Bhutani, K. (2012). Antioxidant activity of a new phenolic glycoside from *Lagenaria siceraria* Stand. fruits. *Food Chemistry*, 132, 244–251. <https://doi.org/10.1016/j.foodchem.2011.10.063>
- Montalti, M., Battistelli, G., Cantelli, A., & Genovese, D. (2014). Photo-tunable multicolour fluorescence imaging based on self-assembled fluorogenic nanoparticles. *Chemical Communications*, 50, 5326-5329. <https://doi.org/10.1039/c3cc48464e>
- Obrenovich, E. M., Li, Y., Parvathaneni, K., Yendluri, B., Palacios, H. H., Leszek, J., & Aliev, G. (2011). Antioxidants in health, disease and aging. *CNS & Neurological*



Disorders - Drug Targets, 10, 192–207.  
<https://doi.org/10.2174/187152711794480375>

Okuyama, K. (2008). Revisiting the molecular structure of collagen. *Connective Tissue Research*, 49, 299–310. <https://doi.org/10.1080/03008200802325110>

Ozdal, T., Capanoglu, E., & Altay, F. (2013). A review on protein–phenolic interactions and associated changes, *Food Research International*, 51, 954–970. <https://doi.org/10.1016/j.foodres.2013.02.009>

Patel, A. R., Heussen, P. C. M., Hazekamp, J., Drost, E., & Velikov, K. P. (2012). Quercetin loaded biopolymeric colloidal particles prepared by simultaneous precipitation of quercetin with hydrophobic protein in aqueous medium. *Food Chemistry*, 133, 423–429. <https://doi.org/10.1016/j.foodchem.2012.01.054>

Rampazzo, E., Bonacchi, S., Juris, R., Genovese, D., Prodi, L., Zaccheroni, N., & Montalti, M. (2018). Dual-mode, anisotropy-encoded, ratiometric fluorescent nanosensors: towards multiplexed detection. *Chemistry–A European Journal*, 24, 16743–16746. <https://doi.org/10.1002/chem.201803461>

Rault, I., Frei, V., Herbage, D., Abdul-Malak, N., & Huc, A. (1996). Evaluation of different chemical methods for cross-linking collagen gel, films and sponges. *Journal of Materials Science: Materials in Medicine*, 7, 215–221. <https://doi.org/10.1007/BF00119733>

Shavandi, A., Bekhit, A. E.-D. A., Saeedi, P., Izadifar, Z., Bekhit, A. A., & Khademhosseini, A. (2018). Polyphenol uses in biomaterials engineering. *Biomaterials*, 167, 91–106. <https://doi.org/10.1016/j.biomaterials.2018.03.018>

Strauss, G., & Gibson, S. M. (2004). Plant phenolics as cross-linkers of gelatin gels and gelatin-based coacervates for use as food ingredients. *Food Hydrocolloids*, 18, 81–89. [https://doi.org/10.1016/S0268-005X\(03\)00045-6](https://doi.org/10.1016/S0268-005X(03)00045-6)

- Sung, H. W., Huang, D. M., Chang, W. H., Huang, R. N., & Hsu, J. C. (1999). Evaluation of gelatin hydrogel crosslinked with various crosslinking agents as bioadhesives: in vitro study. *Journal of Biomedical Materials Research*, 46, 520–530. [https://doi.org/10.1002/\(SICI\)1097-4636\(19990915\)46:4<520::AID-JBM10>3.0.CO;2-9](https://doi.org/10.1002/(SICI)1097-4636(19990915)46:4<520::AID-JBM10>3.0.CO;2-9)
- van Wachem, P. B., Zeeman, R., Dijkstra, P. J., Feijen, J., Hendriks, M., Cahalan, P. T., & van Luyn, M. J. A. (1999). Characterization and biocompatibility of epoxy-crosslinked dermal sheep collagens. *Journal of Biomedical Materials Research*, 47, 270–277. [https://doi.org/10.1002/\(sici\)1097-4636\(199911\)47:2<270::aid-jbm18>3.0.co;2-d](https://doi.org/10.1002/(sici)1097-4636(199911)47:2<270::aid-jbm18>3.0.co;2-d)
- Wang, W., Sun, C., Mao, L., Ma, P., Liu, F., Yang, J., & Gao, Y. (2016). The biological activities, chemical stability, metabolism and delivery systems of quercetin: A review. *Trends in Food Science & Technology*, 56, 21-38. <https://doi.org/10.1016/j.tifs.2016.07.004>
- Zhang, X., Do, M. D., Casey, P., Sulistio, A., Qiao, G. G., Lundin, L., Lillford, P., & Kosaraju, S. (2010). Chemical cross-linking gelatin with natural phenolic compounds as studied by high-resolution NMR spectroscopy. *Biomacromolecules*, 11, 1125–1132. <https://doi.org/10.1021/bm1001284>
- Zhang, Y., Yang, Y., Tang, K., Hu, X., & Zou, G. (2008). Physicochemical characterisation and antioxidant activity of quercetin-loaded chitosan nanoparticles. *Journal of Applied Polymer Science*, 107, 891–897. <https://doi.org/10.1002/app.26402>

608 **Table 1.** Quercetin content of the functionalized films as a function of its theoretical  
609 content.

Theoretical (T) and Experimental (E) quercetin content					
Sample	T (wt%)	E (wt%)	Sample	T (wt%)	E (wt%)
DMSO 05	1.0	1.0	EtOH 05	1.0	0.4
DMSO 1	2.0	2.0	EtOH 1	2.0	0.8
DMSO 15	2.9	2.9	EtOH 15	2.9	1.2
DMSO 2	3.8	3.8	EtOH 2	3.8	1.8

610

611

612 **Table 2.** Denaturation temperatures ( $T_D$ ) and enthalpies ( $\Delta H_D$ ) of EtOH films recorded  
 613 through DSC measurements.

<i>Sample</i>	$T_D$ ( $^{\circ}C$ )	$\Delta H_D$ (J/g)
EtOH 0	100±1	28±1
EtOH 1	102±1	14±1
EtOH 15	98±1	18±1
EtOH 2	99±1	14±1

614

615

**Table 3.** Strain at Break,  $\sigma_b$ , Stress at Break,  $\epsilon_b$ , and Young's Modulus, E, of EtOH films. Each value is the mean of at least seven determinations and is reported with its standard deviation.

sample	E (MPa)	$\sigma_b$ (MPa)	$\epsilon_b$ (%)
EtOH 0	$1.5 \pm 0.2$	$0.28 \pm 0.05^a$	$100 \pm 20^a$
EtOH 05	$1.3 \pm 0.4$	$0.54 \pm 0.08$	$135 \pm 20^b$
EtOH 1	$1.8 \pm 0.6$	$1.1 \pm 0.2^a$	$202 \pm 29^a$
EtOH 15	$1.9 \pm 0.6$	$1.4 \pm 0.1^a$	$238 \pm 10^{a,b}$
EtOH 2	$1.4 \pm 0.8$	$0.4 \pm 0.2^a$	$109 \pm 30^a$

$\sigma_b$  : <sup>a</sup> EtOH 0 vs EtOH 05, EtOH 1, EtOH 15; EtOH 1 vs EtOH 05; EtOH 15 vs EtOH 05; EtOH 2 vs EtOH 1, EtOH 15 (  $p < 0.001$ ). <sup>b</sup> EtOH 15 vs EtOH 1 (  $p < 0.05$ )

$\epsilon_b$  : : <sup>a</sup> EtOH 0 vs EtOH 1, EtOH 15; EtOH 1 vs EtOH 05; EtOH 15 vs EtOH 05; EtOH 2 vs EtOH 1, EtOH 15 (  $p < 0.001$ ). <sup>b</sup> : EtOH 05 vs EtOH 0; EtOH 15 vs EtOH 1 (  $p < 0.05$ )

**Figures Captions.**

**Figure 1-** Absorption spectra of DMSO (a) and EtOH (b) gelatin-quercetin film solutions (0.4 mg/mL in water/ethanol 1:1).

**Figure 2-** TGA plots of (a) EtOH films and (b) DMSO films. The insets show an enlargement of the final parts of the plots.

**Figure 3-** Swelling curves of (a) EtOH films and (b) DMSO films. Each value was determined in triplicate. Standard deviations are comprised into the size of the symbols.

**Figure 4-** DSC thermograms recorded from dried EtOH 0 and EtOH 1 films show the presence of an endothermic peak due to collagen triple helix denaturation.

**Figure 5-** X-rays diffraction patterns of EtOH films showing the presence of the 1.1 nm reflection; which is absent in DMSO films.

**Figure 6-** Typical stress-strain curves of EtOH gelatin films at different quercetin content.

**Figure 7-** Quercetin release for each refresh (a), and cumulative release (b) expressed in mg. (c, d) cumulative release expressed as % of the initial content from DMSO (c) and EtOH (d) films.

**Figure 8-** Antiradical activity, expressed as % RSA, of the different samples and pure quercetin toward DPPH•. Bars represent the mean  $\pm$  SD of two independent measurements.

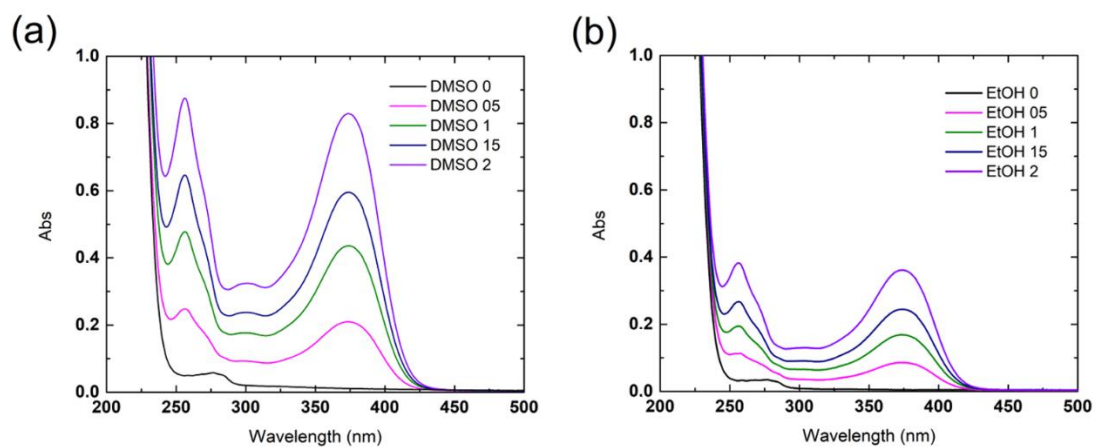


Figure 1

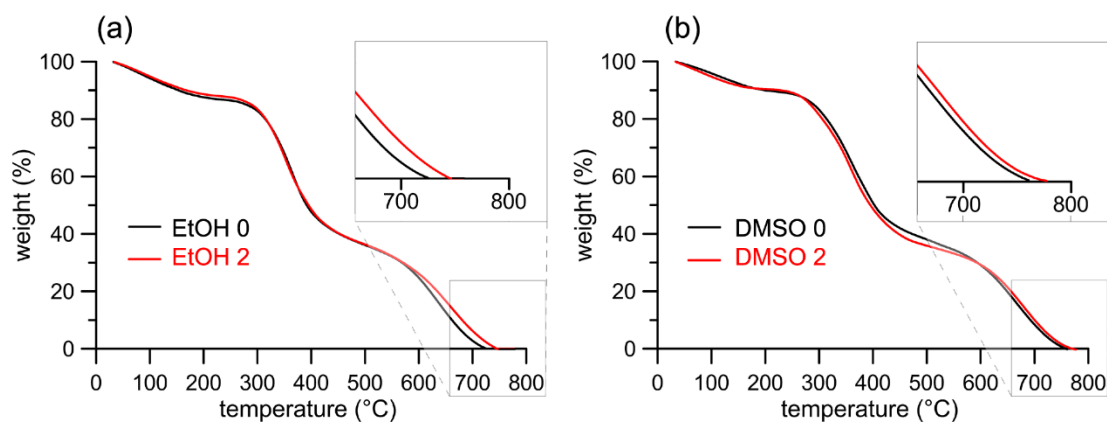


Figure 2

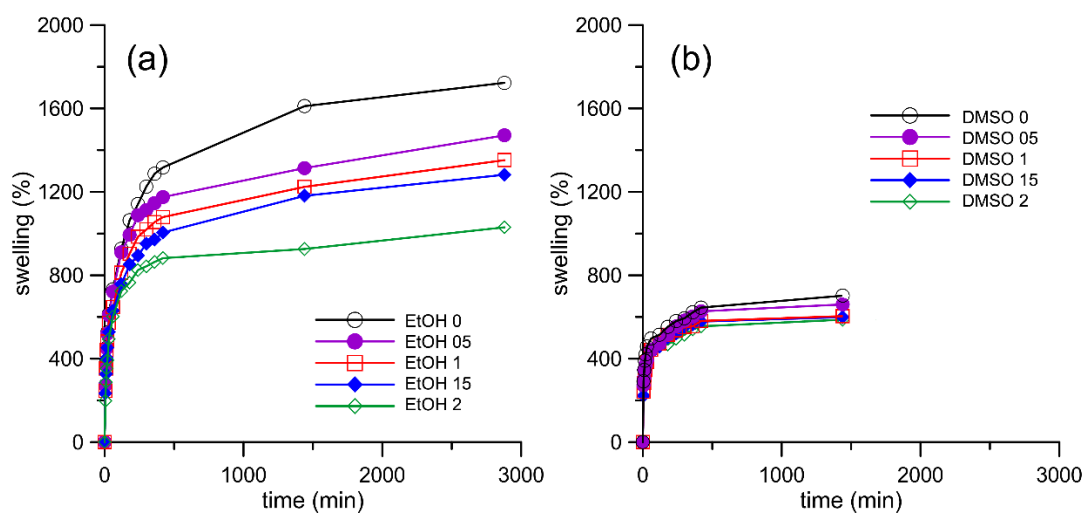


Figure 3

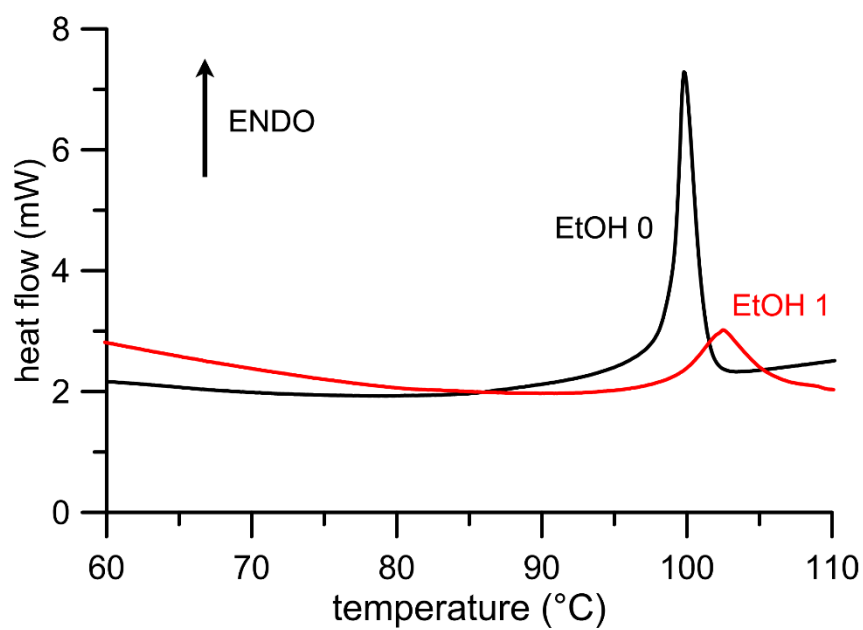


Figure 4

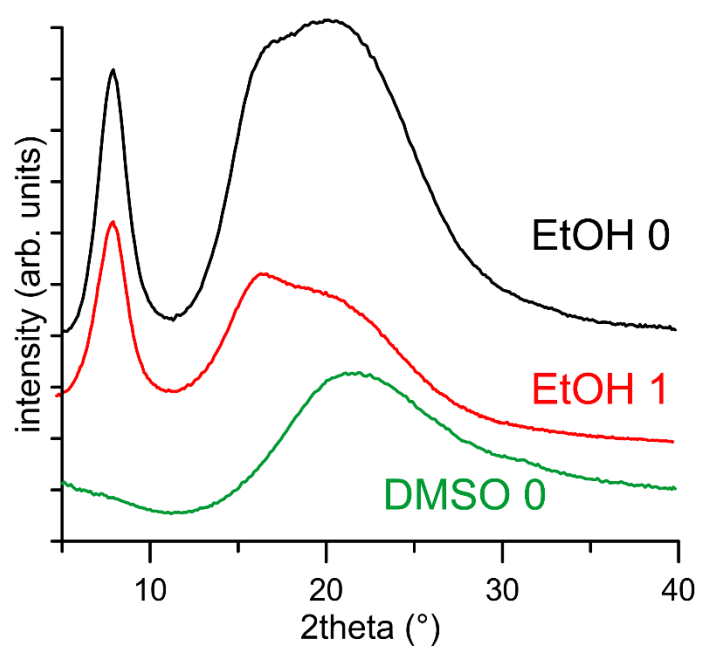


Figure 5



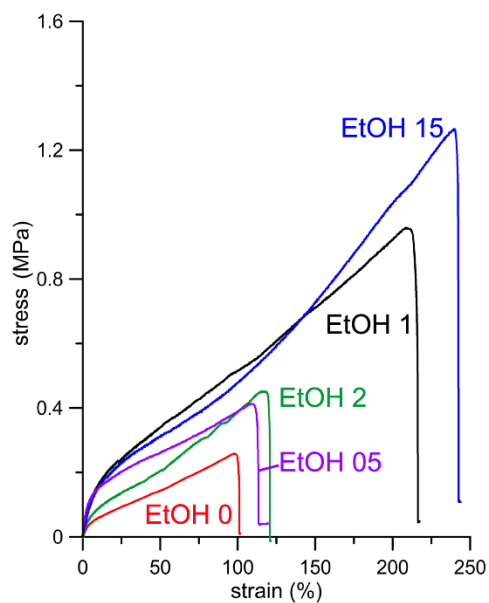


Figure 6

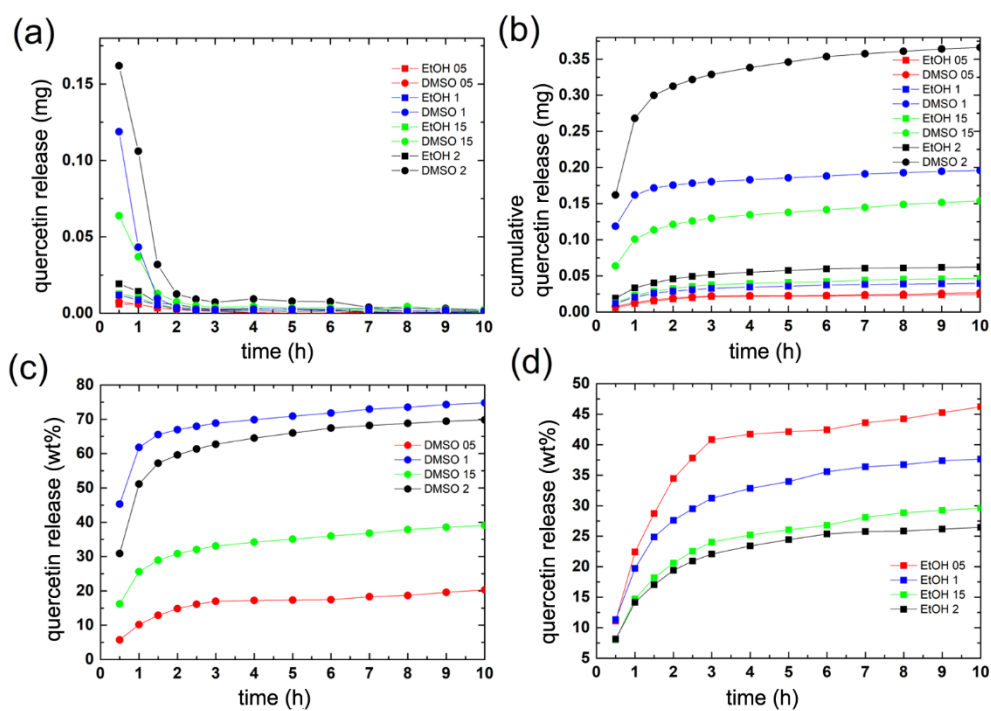


Figure 7

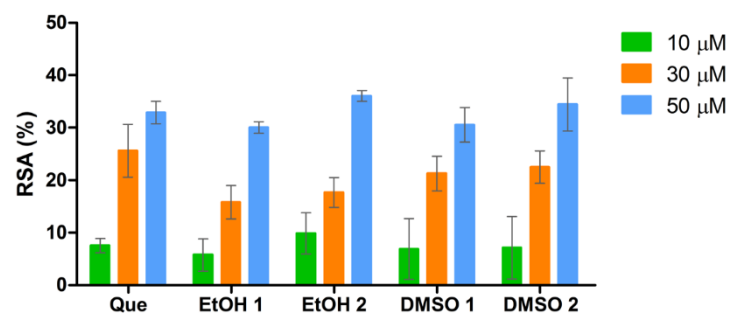


Figure 8